Radiotherapy and Oncology 177 (2022) 164–171

Contents lists available at ScienceDirect

Radiotherapy and Oncology

journal homepage: www.thegreenjournal.com

Original Article

Dose response modelling of secretory cell loss in salivary glands using PSMA PET

Vineet Mohan [a,b], Natascha M. Bruin [a,b], Roel J.H.M. Steenbakkers [c], Walter Noordzij [d], Chris H.J. Terhaard [e], Bart de Keizer [f], Abrahim Al-Mamgani [a], Jeroen B. van de Kamer [a], Jan-Jakob Sonke [a], Wouter V. Vogel [a,b,*]

[a] Department of Radiation Oncology; [b] Department of Nuclear Medicine, The Netherlands Cancer Institute, Amsterdam; [c] Department of Radiation Oncology; [d] Department of Nuclear Medicine and Molecular Imaging, University Medical Center Groningen, University of Groningen, Groningen; [e] Department of Radiotherapy; and [f] Department of Nuclear Medicine and Radiology, University Medical Center Utrecht, Utrecht, the Netherlands

ARTICLE INFO

Article history:
Received 11 June 2022
Received in revised form 7 October 2022
Accepted 31 October 2022
Available online 8 November 2022

Keywords:
Head-and-neck cancer
Dose response
Salivary glands
Toxicity
PET
PSMA

ABSTRACT

Background and purpose: Xerostomia remains a common side effect of radiotherapy (RT) for patients with head and neck (H&N) cancer despite advancements in treatment planning and delivery. Secretory salivary gland cells express the prostate-specific membrane antigen (PSMA), and show significant uptake on PET scans using ^{68}Ga/^{18}F-PSMA-ligands. We aimed to objectively quantify the dose–response of salivary glands to RT using PSMA PET.

Methods and materials: 28H&N cancer patients received RT with 70 Gy in 35 fractions over 7 weeks. PSMA PET/CT was acquired at baseline (BL), during treatment (DT) and at 1-&6-months post-treatment (PT_{1M}/PT_{6M}). Dose, BL- PT_{1M}- and PT_{6M}-SUV were extracted for every voxel inside each parotid (PG) and submandibular (SMG) gland. The $PT_{1M/6M}$ data was analysed using a generalised linear mixed effects model. Patient-reported xerostomia and DT-PSMA loss was also analysed.

Results: Dose had a relative effect on BL SUV. For a population average gland (BL-SUV of 10), every 1 Gy increment, decreased the PT_{1M}/PT_{6M}-SUV by 1.6 %/1.6 % for PGs and by 0.9 %/1.8 % for SMGs. TD_{50} of the population curves was 26.5/31.3 Gy for PGs, and 22.9/27.8 Gy for SMGs at PT_{1M} /PT_{6M}. PSMA loss correlated well with patient-reported xerostomia at DT/PT_{1M} (Spearman's ρ = -0.64, −0.50).

Conclusion: A strong relationship was demonstrated between radiation dose and loss of secretory cells in salivary glands derived using PSMA PET/CT. The population curve could potentially be used as a dose planning objective, by maximising the predicted post-treatment SUV. BL scans could be used to further tailor this to individual patients.

Salivary gland toxicity, and its manifestation as xerostomia or the subjective feeling of a dry mouth, is a common side effect in head and neck (H&N) cancer patients treated with radiation and can result in serious detriment in the quality of life. Despite advancements in parotid gland (PG) sparing, patient reported xerostomia remains high[1,2]. Salivary gland toxicity has classically been assessed with sialometry or salivary gland flow rates, physician rated scores, and ^{99m}Tc scintigraphy[3]. These techniques are often subjective in nature, lack spatial information, suffer from poor repeatability or are found to correlate poorly with the patient's experience of xerostomia[4–7]. Current recommended dose constraints for PGs and submandibular glands (SMGs) are derived from studies that employed the aforementioned techniques[8,9]. However, in clinical practice these constraints are often overridden to achieve sufficient target coverage. In order to predict and assess xerostomia at various dose levels, a more objective measurement method and granular dose–response model are required.

The secretory cells of salivary glands express the prostate-specific membrane antigen (PSMA) and exhibit substantial uptake on positron emission tomography/computed tomography (PET/CT) scans of diagnostic PSMA ligands (usually labelled with ^{68}Ga or ^{18}F) [10]. These PET tracers are highly sensitive and specific, and are typically used in the staging of prostate cancer. Recently, it was

Abbreviations: BL, Baseline; CT, Computed tomography; DT, During treatment; EBRT, External beam radiotherapy; FDG, fluoro-2-deoxyglucose; GRIX, Groningen radiotherapy-induced xerostomia; H&N, Head and neck; PET, Positron emission tomography; PG, Parotid gland; PSMA, Prostate-specific membrane antigen; $PT_{1M/6M}$, 1/6-month(s) post-treatment; RT, Radiotherapy; SMG, Submandibular gland; SUV, Standardized uptake value.

* Corresponding author at: Departments of Nuclear Medicine and Radiation Oncology, The Netherlands Cancer Institute, Plesmanlaan 121, 1066 CX Amsterdam, the Netherlands.

E-mail address: w.vogel@nki.nl (W.V. Vogel).

https://doi.org/10.1016/j.radonc.2022.10.038
0167-8140/

demonstrated that salivary gland tissue that is damaged by radiotherapy (RT) loses its ability to take up PSMA-ligands.[11]. By virtue of directly measuring this local loss of signal in 3D with high contrast and relatively high resolution, PSMA PET is potentially a strong candidate for objective and quantitative dose–response assessment.

The primary purpose of this work was to derive and model the post-treatment dose–response of PGs and SMGs to radiation using PSMA PET. The secondary objective was to correlate PSMA uptake changes with patient reported xerostomia, and explore at what stage during treatment PSMA loss becomes apparent.

Methods

The Medical Ethics Committee of the Netherlands Cancer Institute (CCMO trial registration NL60569.031.17) approved the study protocol. The study was conducted in accordance with the Declaration of Helsinki. Written and oral informed consent was obtained from all patients prior to study entry.

Patients

The prospective study included 30 patients with head and neck cancer treated in The Netherlands between 2017 and 2021 from 3 centres (Netherlands Cancer Institute, University Medical Center Groningen, and University Medical Center Utrecht). Eligibility criteria included patients newly diagnosed with head and neck squamous cell carcinomas (cTx-4 N0-3 M0) and accepted for primary or postoperative radiotherapy. The treatment regimen to be followed was conventionally fractionated external beam (photon or proton) radiotherapy (EBRT) with curative intent, delivered in 35 fractions of 2 Gy in 6–7 weeks. Patients receiving concurrent chemoradiotherapy were also to be included.

Data acquisition

Patients received PSMA PET/CT scans at 4 time points; at baseline (BL) a few days before treatment commenced, at a variable time point between week 2 and 7 during treatment (DT), 1-month post-treatment (PT_{1M}), and 6-month post-treatment (PT_{6M}). Patients were scanned with either [^{68}Ga]Ga-PSMA-11 or [^{18}F]F-PSMA-1007as the PET tracer. At each time point, patients were asked to fill in the Groningen Radiotherapy-Induced Xerostomia (GRIX) questionnaire[12]. For each patient, tracer choice and PET scanner were fixed across all time points. Each institute used EARL accredited PET scanners. The image acquisition procedure was identical at each time point and is described as follows.

Patients were adequately hydrated, followed by intravenous administration of 50 MBq [^{68}Ga]Ga-PSMA or 100 MBq [^{18}F]F-PSMA. After an incubation time of 45–60 minutes patients were positioned in the PET scanner in treatment position using their immobilization masks. A low-dose CT scan of the head and neck region was acquired with 1–2 mm slices. A PET scan of the same region was acquired in 4–12 minutes for 1–2 bed positions according to scanner characteristics from different centres. The scan was reconstructed iteratively to 2x2x2 mm^3 voxels with attenuation correction according to EARL specifications. The DT, PT_{1M} and PT_{6M} PET scans were normalised to the BL scan by measuring the SUV_{mean} in the muscles at the back of the neck.

Data analysis

The planning CT (pCT) acquired for radiotherapy served as the reference anatomy for each patient. The CT scan of the PET/CT of each time point was first rigidly and then deformably registered to the pCT using a validated, in-house developed, cubic B-spline deformable registration algorithm[13]. This was done separately for each individual PG and SMG by using the associated delineation as a mask for the registration. The resulting deformation vector field was subsequently applied to the PET scan, which was then resampled to the 3x3x3 mm^3 grid of the RT dose field. To ensure conservation of the total PET signal within the gland before and after undergoing the deformation, each voxel's value was divided by the Jacobian determinant of the deformation vector at that voxel (which represents the change in volume of the voxel). The SUV of each voxel at each time point, as well as the physical dose it was planned to received, was extracted for each gland of each patient. In the case of replanning during treatment, the new dose field was deformed to the anatomy of the original pCT and averaged with the original dose proportional to the number of fractions delivered with each plan. For proton therapy dose fields, a constant relative biological effectiveness of 1.1 was assumed.

Statistical analysis

Statistical analysis was done using R v4.1.1[14]. Generalised linear mixed effects models of the relationship between PT_{1M}/PT_{6M} SUV, dose, and BL SUV were created using the lme4 package[15]. Graphical plots were generated using the ggplot2 and interactions package[16,17]. By using a mixed effects model, correlations between multiple repeated measurements (voxels) from each patient were accounted for. Dose and BL SUV were centred at 25 Gy and 10 SUV (for better interpretability of coefficients) and entered as fixed effects, along with an interaction term between them. The model was fit with full random effects, thus allowing the intercept and the coefficient of each term to vary per patient within a normal distribution centred on the population coefficient estimate. A log link function was chosen to fit the shape of the data and constrain the predicted output, and a gaussian variance structure was assumed for the response. Four models were generated, one for each gland type (PG and SMG) and time point (PT_{1M} and PT_{6M}). Statistical significance of covariates was determined using

Table 1
Patient characteristics.

No. of Patients	28
Age (Years)	
Median	63
Range	47 – 81
Sex	
Male	23
Female	5
Site	
Hypopharynx	2
Larynx	2
Oral Cavity	5
Oropharynx	14
Supraglottic	3
Unknown	2
T Stage	
T0	2
T1	6
T2	7
T3	10
T4	3
Systemic Therapy	
Concurrent	12
Only RT	16
Treatment	
Photons	23
Protons	5
PET Tracer	
^{68}Ga	22
^{18}F	6

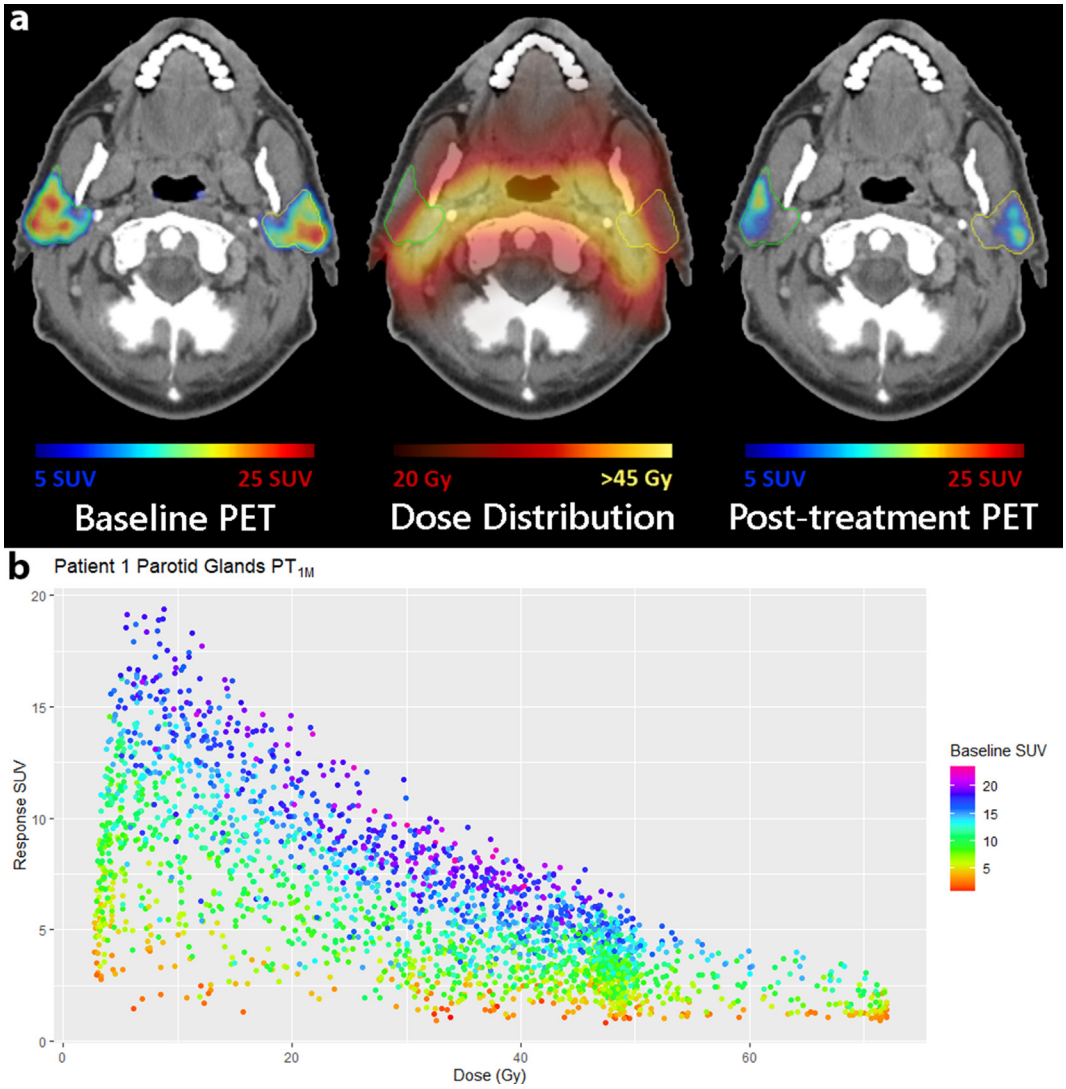

Fig. 1. (a) Baseline and 1-month post-treatment PET scans and dose distribution overlaid on the planning CT of patient 1. The regions of the parotid glands that received higher dose exhibit the greatest loss of signal. (b) Baseline SUV, 1-month post-treatment SUV and dose of each voxel, depicted as individual points, from patient 1's parotid glands. The slope appears increasingly negative at higher levels of baseline SUV.

likelihood ratio tests conducted against reduced models without the covariate in question. In general, defining a coefficient of determination (R^2) for these types of models is not straightforward. The R^2 values reported here were computed by comparing residual variance of the full model against the residual variance of a fixed intercept-only model[18]. To allow comparisons to other models in literature, we calculate the dose at which the post-treatment SUV reaches 50 % of its original baseline value (TD_{50}).

For the DT timepoint analysis, patients were divided into 3 groups based on which week of the treatment the DT scan was made; Group 1 (week 2–3), Group 2 (week 4–5), Group 3 (week 6–7). The relative change (Δ_{rel}) in total PSMA uptake of all glands (SUV_{tot}) from BL was calculated for each group. A more in-depth analysis and discussion of the DT timepoint is available in the supplementary material.

The change in the dry mouth related GRIX questionnaire scores (questions 1–9), as well as relative change in SUV_{tot} of all glands from BL to DT, PT_{1M} and PT_{6M} were derived for each patient. Spearman's ρ was then calculated between the ΔGRIX scores and $\Delta_{rel}SUV_{tot}$.

Results

Two patients were unevaluable due to incomplete scans and incorrect PET reconstruction protocol. Of the 28 evaluable patients, 18 were from the Netherlands Cancer Institute, 7 from the University Medical Center Groningen, and 3 from the University Medical Center Utrecht. Twenty-two patients were scanned with [^{68}Ga]Ga-PSMA and 6 with [^{18}F]F-PSMA. Twenty-three patients were treated with volumetric modulated arc therapy and 5 with intensity modulated proton therapy. Three patients underwent replanning during treatment. Twelve patients received concurrent systemic therapy (9 cisplatin, 2 cetuximab and 1 olaparib). A summary of patient characteristics can be found in Table 1, and a detailed version can be found in Suppl. Table I. The average BL SUV and mean dose for all 28 patients was 9.9 and 23.7 Gy for PGs, and 10.8 and 51.4 Gy for SMGs respectively. The median and interquartile range (IQR) of the normalisation factors were 0.99 (0.94–1.02) for the DT scans, 0.93 (0.88–0.96) for PT_{1M} and 0.95 (0.91–1.00) for PT_{6M}. Eleven patients were assigned to Group 1, 10 to Group 2, and 7 to Group 3 based on their DT scan.

Table 2
Coefficient estimates on the log-link scale along with their standard errors (SE) and the standard deviation (SD) of their respective random effects, as well as the exponentiated coefficients on the response scale from the 4 dose response models.

Model	Intercept (α)				Baseline SUV (β_1)				Dose (β_2)				Interaction (β_3)				R^2
	Link Scale	SE	SD	Response Scale	Link Scale	SE	SD	Response Scale	Link Scale	SE	SD	Response Scale	Link Scale	SE	SD	Response Scale	
PT_{1M} PG	1.63†	0.05	0.37	5.12	0.078†	0.004	0.028	1.081	−0.016†	0.001	0.010	0.984	−0.0005†	0.0001	0.0009	0.9995	0.85
PT_{6M} PG	1.71†	0.05	0.41	5.53	0.083†	0.005	0.041	1.087	−0.016†	0.001	0.010	0.984	−0.0001	0.0001	0.0011	0.9999	0.82
PT_{1M} SMG	1.59†	0.06	0.33	4.90	0.077†	0.005	0.025	1.080	−0.009†	0.001	0.005	0.991	−0.0003†	0.0001	0.0005	0.9997	0.80
PT_{6M} SMG	1.66†	0.05	0.29	5.26	0.085†	0.007	0.039	1.089	−0.018†	0.001	0.006	0.982	−0.0009†	0.0002	0.0008	0.9991	0.80

Model equations given by $\log(E[y]) = \alpha + \beta_1{}^*(\text{Baseline SUV-10}) + \beta_2{}^*(\text{Dose-25}) + \beta_3{}^*(\text{Baseline SUV-10})^*(\text{Dose-25})$.
† $p < 0.001$. p-value of interaction term in PT_{6M} PG > 0.05.

Of the 28 patients evaluated, 1 missed their DT scan (from Group 2), 2 missed their PT_{1M} scans, and 5 others missed their PT_{6M} scans and were thus excluded from the respective analyses/-models. One patient's left PG (from Group 3) was fully excluded from the dose response analysis due to its PSMA uptake on the BL scan diffusing into the nearby tumour. Seven SMGs from 4 patients were also excluded from the PT_{6M} model either due to these glands being resected prior to the PT_{6M} scan or due to implausible registration results. Despite missing their scans, GRIX questionnaire scores were still available for some patients at the timepoint in question. GRIX questionnaires were unavailable for 1 patient at baseline, 2 at DT, 3 at PT_{1M} and 2 at PT_{6M}. Descriptive statistics for SUV_{tot} excluded patients with missed scans and ineligible glands. Patients who missed scans or had ineligible glands, or had missing GRIX scores were excluded from the calculation of Spearman's ρ.

BL and PT_{1M} PSMA PET scan of patient 1, along with their respective dose distribution can be seen in Fig. 1a. The voxel data once extracted from these scans can be represented graphically, as seen in Fig. 1b.

The estimated population coefficients/fixed effects for each of the models are shown in Table 2. The coefficients, once exponentiated and on the response scale, can each be interpreted individually by setting the other variables to the shifted zero. For example, assuming a BL SUV of 10 (which is approximately the population average for PGs and SMGs) and a dose of 25 Gy, the predicted PT_{1M} SUV of a PG voxel is 5.12, which is the intercept. Assuming a BL SUV of 10, for every increase in 1 Gy the PT_{1M} SUV of a PG voxel decreases by 1.6 %. Assuming a dose of 25 Gy, an increment in BL SUV of 1, increases the PT_{1M} SUV of a PG voxel by 8.1 %. The magnitude of the interaction terms is near negligible in most cases and is only relevant at high values of dose and BL SUV. If for example, the BL SUV of a voxel is 15 and the dose it receives is 35 Gy, the interaction term reduces the predicted PT_{1M} SUV of a PG voxel by merely 0.15. Treatment modality and systemic therapy were tested as fixed effects for each of the models but were found to have no significant effect ($p = 0.1–0.9$).

The 4 models are represented graphically in Fig. 2. The exponential decay is noticeably steeper at higher levels of BL SUV. The TD_{50} of PGs is 26.5 Gy at PT_{1M} and 31.3 Gy at PT_{6M} assuming a BL SUV of 10. For SMGs this is at 22.9 Gy for PT_{1M} and 27.8 Gy at PT_{6M} (and 21 Gy and 27.2 Gy at the SMG mean BL SUV of ~ 11). An overlaid comparison of all 4 models is presented in Suppl. Figs. 1a-c. The PT_{1M} SMG response exhibited a lower intercept and a shallower decay curve than the other 3 models. Although the models were fitted to slightly different patient cohorts, the difference between the PT_{1M} and PT_{6M} SMG response persisted when fitted to a common reduced dataset (Suppl. Fig. 1d).

The estimated SDs of the interpatient variation (random effects) are reported in Table 2 and a plot of the random effects for all patients can be found in Suppl. Fig. 2a-d. As an example, at PT_{1M} for PGs, at a BL SUV of 10 and dose of 25 Gy, we expect 95 % of the predicted SUV of all patients to range from 2.5 – 10.7 (variation in intercept from Table 2). Similarly, the 95 % range of the effect of an increment of 1 BL SUV was from 2.4 – 14.2 %, and of 1 Gy was from 0 – 3.5 %. Patient-specific coefficients for dose were fairly negatively correlated with their intercepts, implying that patients with shallow/flat dose–response curves still exhibited large amounts of PSMA loss even in low dose regions. The median (IQR) TD_{50} for individual patients was 27.8 Gy (20.1–34.9) and 32.2 Gy (21.2–41.8) for PGs at PT_{1M} and PT_{6M}, and 31.4 Gy (4.3–42.5) and 28.5 Gy (16.6 – 34.5) for SMGs at PT_{1M} and PT_{6M} respectively. Individual patient-specific fits from the 4 models with BL SUV held at each patient's gland

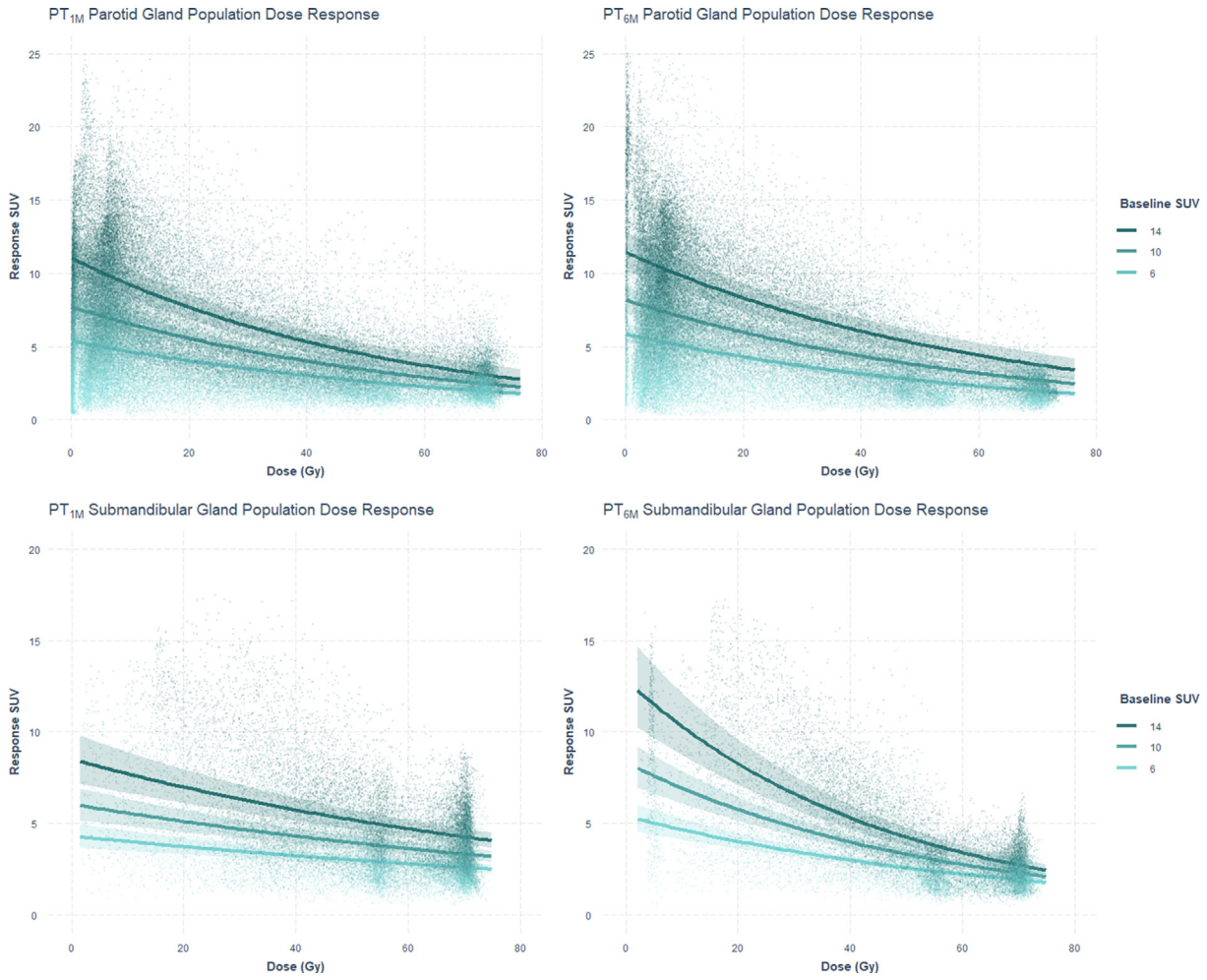

Fig. 2. Population dose response curves for the parotid and submandibular glands at 1 and 6-months post-treatment, plotted for baseline SUV values of 6, 10 and 14 and with their respective 95% confidence intervals. Individual dots represent voxels from all patients and the colour gradient represents baseline SUV.

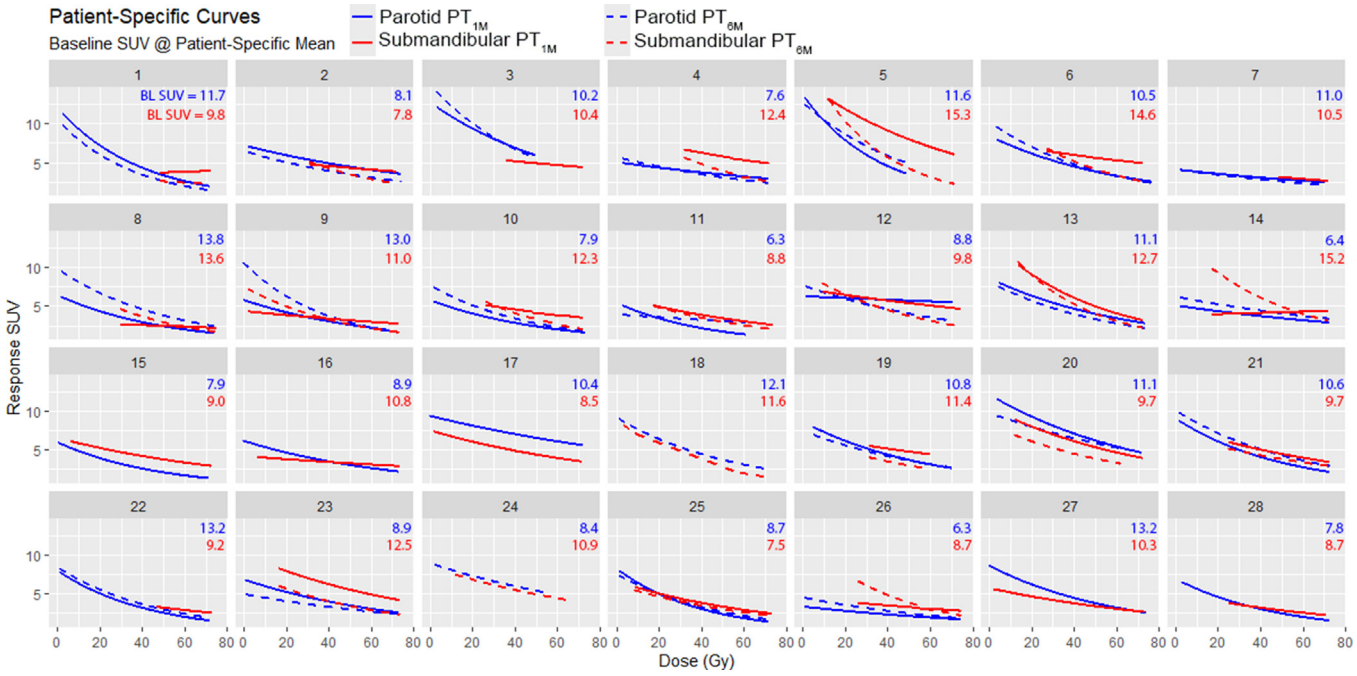

Fig. 3. Patient-specific curves for all glands and time points, plotted at each patient's gland type's baseline SUV_{mean}.

specific SUV_{mean} can be seen in Fig. 3. The adjusted intraclass correlation coefficient for the models was between 0.07–0.09.

Patient-specific plots with BL SUV at each patient's SUV_{mean} ± 1 SD can be seen in Suppl. Fig. 3a-d. Differences between population and patient-specific fits for each patient, with BL SUV at each patient's SUV_{mean} are shown in Suppl. Fig. 4a-d.

The median $\Delta_{rel}SUV_{tot}$ from BL to DT was −0.30 (n = 11) for Group 1, −0.32 (n = 9) for Group 2, and −0.41 (n = 6) for Group 3. Dose response analysis and discussion for the DT timepoint can be found in supplementary material.

On a scale of 0–100, the median (IQR) GRIX dry mouth score was 3.7 (0–13.9, n = 27) at baseline, 29.6 (18.5–51.9, n = 26) at DT, 37.0 (13.9–60.2, n = 25) at PT_{1M} and 33.3 (18.5–44.4, n = 26) at PT_{6M}. Spearman's ρ between ΔGRIX scores and $\Delta_{rel}SUV_{tot}$ was −0.64 (n = 26, p < 0.01) at DT, −0.50 (n = 22, p = 0.02) at PT_{1M} and −0.28 (n = 19, p = 0.09) at PT_{6M}. When comparing ΔGRIX scores with $\Delta_{rel}SUV_{tot}$ of PGs only this was −0.64 (n = 26, p < 0.01) at DT, −0.42 (n = 22, p = 0.05) at PT_{1M} and −0.35 at PT_{6M} (n = 19, p = 0.14). For SMGs only this was −0.63 (n = 26, p < 0.01), −0.55 (n = 22, p < 0.01) at PT_{1M} and −0.25 (n = 19, p = 0.30) and PT_{6M}. Comparing the mean dose to the glands with the scores, Spearman's ρ ranges from 0.10-0.33 (p > 0.14). Baseline PSMA SUV_{tot} did not correlate with baseline GRIX scores.

Discussion

To our knowledge this is the first time the dose response for loss of secretory cells in PGs and SMGs to EBRT has been characterised using PSMA PET/CT. The dose response at the 1-month and 6-months post-treatment followed a log decay curve with dose having a relative effect on baseline SUV. Substantial PSMA loss was measurable in the second week of RT already. PSMA loss correlated well with patient-reported xerostomia initially but weakened over time.

Efforts to assess the dose–response of salivary glands using PET have been reported previously. Buus et al.[19] explored the use of dynamic [^{11}C]methionine PET, a tracer that measures protein synthesis as a marker of functional cells, to derive the dose response of PGs in 12H&N cancer patients at the voxel level; an approach similar to this study. They modelled the post-treatment PET response voxels and planned dose distribution using a sigmoid curve and arrived at a population TD_{50} of 30 Gy and threshold dose of 16 Gy. Similarly, they also found significant variation between patients (individual patient TD_{50} ranged from 7-50 Gy). They however did not make use of a pre-treatment PET, without which the sensitivity of different baseline levels of functional activity to dose could not be characterised. The patients also received their scans at variable time points between 8–54 months after RT. Moreover, dynamic PET with [^{11}C]methionine is comparatively laborious and complex in part due to invasive blood sampling and the short half-life of ^{11}C.

Several studies have investigated the effect of dose on uptake of the ubiquitous tracer, [^{18}F]fluoro-2-deoxyglucose (FDG). Roach et al.[20] reported that SUV_{mean} decreased linearly, and SUV_{max} sigmoidally in PGs as a function of mean dose. Cannon et al.[21] investigated this relationship further on a voxel level, and also noted the moderating effect of baseline SUV on the effect of dose, by using SUV-weighted dose in their analysis. Van Dijk et al.[22] found that the inclusion of baseline [^{18}F]FDG PET features improved the prediction of xerostomia at 12 months post-treatment. Wilkie et al.[23] verified these findings independently and also observed that post-treatment PET features improved prediction further. Elhalawani et al.[24] also found predictive effects for xerostomia from post-treatment PET, but failed to find any from pre-treatment PET. They also contrarily noted that while SUV decreased between pre- and post-treatment, this did not occur in a dose-dependent manner.

The problem with [^{18}F]FDG PET analyses lies in the lack of sensitivity and specificity of the tracer to the salivary glands, resulting in low dynamic range, along with the confounding effect of radiation-induced inflammation, which can lead to an increase in [^{18}F]FDG uptake. As an example of this, Mouminah et al.[25] found that SUV_{mean} increased in PGs by 0.12 SUV on average, when compared to baseline for patients treated with photons. PSMA being more specific and sensitive as a tracer, is superior in its ability to measure changes due to dose. Due to its higher dynamic range of values, the effect of dose can be studied at finer gradations of baseline levels too. The repeatability coefficient of PSMA PET for the parotid glands is on average 23.4 %[26].

Contrary to popular approaches that bin/average data, normalise the response variable to a fraction of baseline function (which has been shown to have poor statistical efficiency[27]), and run a logistic regression in order to fit a sigmoid shaped curve, we instead chose to retain the original response variable as is, incorporate the baseline as a covariate, and run a generalised mixed effect model that accounted for the natural shape of the data as well as all the correlation and variation within and between patients.

An interesting observation is that for all our models, the post-treatment SUV at doses close to 0 Gy exhibited appreciable reduction when compared to the BL SUV value. This varied widely between patients too, as seen in Fig. 3 and Suppl. Fig. 3a-4d. Uncertainties in dose delivery (since only planned dose was used), registration and the repeatability of PET certainly played a role here. One hypothesis is this could be hypersensitivity of the glands to low doses of radiation. Another possibility was systemic therapy, but including this factor failed to improve any of the models. From a mathematical perspective, the intercept could be seen as a systematic 'offset' effect of RT on the salivary gland that varied between patients, after which PSMA loss occurred in a dose dependent manner.

When looking at the dose response curves for the SMGs, the response appeared to improve at PT_{6M} vs PT_{1M} at doses below 30 Gy, and worsen at doses above it (Suppl. Figs. 1a-d). This is in contrast to the PGs, which had very similar population dose response curves at PT_{1M} and PT_{6M}. This behaviour in the SMGs persisted when the models were refitted on a common reduced set of voxels, indicating that the difference itself was not due to a difference in the underlying dataset. However as depicted in Fig. 2c-d, only 10 % of all voxels received less than 25 Gy. Given the sparsity of the data in the low dose region, the uncertainty there is greater. More data of the SMG response in the lose dose region is required for a complete picture.

The TD_{50} of PGs has been derived through scintigraphy and sialometry and is widely reported in literature to hover around 25–40 Gy at 1–12 months after radiotherapy[8,28,29], which fell in line with what we observed. The TD_{50} of SMGs is reported in literature to be around 35–45 Gy, much higher than our observed results, but this may be due to the reported timepoint being 1–2 years post-treatment[9,30].

When comparing PSMA loss to patient-reported xerostomia, correlations were found to be higher at DT than PT_{1M}, and higher at PT_{1M} than PT_{6M}, indicating PSMA loss appears to decouple from xerostomia symptoms as time goes on. Some possible reasons for this could be patients acclimating to their symptoms, or compensation from other minor glands not included in the assessment. Spearman's ρ indicated PSMA loss correlated more with patient reported xerostomia than mean dose did. The magnitude of the correlation was also comparable to those of sialometry studies [6,31].

Our study is naturally not without limitations. The distribution of uptake in sub-regions of the glands was not characterised. Each voxel in the gland was assumed to be an independent functional unit and spatial connectivity was unaccounted for. The models created also did not influence each other; the SMG response did not take into account the function or response of the PGs and vice versa. Neither did the models distinguish between laterality (ipsilateral/contralateral). Xerostomia and salivation are multifactorial; the interplay between glands, such as the compensation by one gland for the dysfunction of another, can play an important role. These trends were not possible to identify in the models we pursued. And lastly, we assumed that PSMA expression was a good surrogate for gland function. While it might be a safe bet that PSMA signal loss is correlated with loss of functional secretory cells, how this translates to saliva production and quality has not been studied. Moreover, while salivary flow and patient-reported xerostomia can recover significantly at 1–2 years post-treatment, it is not known if PSMA expression recovers significantly over time, and if overshoot can occur. Nonetheless, given the correlation between patient reported xerostomia and PSMA loss we found, we still assert its ability to assess xerostomia.

The PSMA PET dose–response models we have presented could find potential use in dose-planning. One could optimise the planning objective to maximise the total predicted post-treatment SUV of a gland, instead of minimising its mean dose. It is possible that for the same mean dose, a different dose distribution could be derived that would result in less PSMA loss, which emphasises the sparing of voxels in the lower dose region, and pushing that dose into regions that already receive a large dose. One could also envision a future wherein a patient receives a PSMA-PET scan prior to RT, upon which a tailor-made dose-plan could be generated by optimising for the distribution and response curves of different baseline values. A during-treatment scan to assess response and adapt to it is also potentially feasible, since our results indicate PSMA loss is demonstrable early in the treatment regimen.

Recently, sparing the purported stem cell rich (SCR) region in the parotid gland has garnered interest as a strategy to preserve parotid gland function [32].Visually, any correlation between PSMA distribution and the SCR region (in the main duct near the junction of the masseter muscle, parotid gland and mandible) is not apparent. Further research is required to investigate if a relation exists between PSMA response and the SCR region, and the role it could play in dose-planning.

Conclusion

In conclusion, we have characterised the dose–response of secretory cell loss in salivary glands to EBRT with PSMA PET using generalised linear mixed models. Dose had a largely relative effect on BL SUV and the response followed an exponential decay curve. PSMA loss correlated well with patient reported xerostomia at DT and PT_{1M}. Significant PSMA loss occurred already in the second/third week of treatment. PSMA PET is a useful objective tool to assess dose–response and its potential in dose-planning should be explored in the future.

Funding

This work was supported by the Dutch Cancer Society KWF [Research Grant: 10606/2016–2].

Ethics approval and consent to participate

The Medical Ethics Committee of the Netherlands Cancer Institute (CCMO trial registration NL60569.031.17) approved the study protocol. The study was conducted in accordance with the Declaration of Helsinki. Written and oral informed consent was obtained from all patients prior to study entry.

Availability of data and material

The datasets generated and analysed for this work may be available from the corresponding author on reasonable request.

Declaration of Competing Interest

The authors declare that they have no known competing financial interests or personal relationships that could have appeared to influence the work reported in this paper.

Appendix A. Supplementary material

Supplementary data to this article can be found online at https://doi.org/10.1016/j.radonc.2022.10.038.

References

[1] Onjukka E, Mercke C, Björgvinsson E, Embring A, Berglund A, Alexandersson von Döbeln G, et al. Modeling of xerostomia after radiotherapy for head and neck cancer: a registry study. Front Oncol 2020;10:1–10. https://doi.org/10.3389/fonc.2020.01647.

[2] Marta GN, Silva V, De Andrade CH, De Arruda FF, Hanna SA, Gadia R, et al. Intensity-modulated radiation therapy for head and neck cancer: Systematic review and meta-analysis. Radiother Oncol 2014;110:9–15. https://doi.org/10.1016/j.radonc.2013.11.010.

[3] Eisbruch A, Rhodus N, Rosenthal D, Murphy B, Rasch C, Sonis S, et al. How should we measure and report radiotherapy-induced xerostomia? Semin Radiat Oncol 2003;13:226–34. https://doi.org/10.1016/S1053-4296(03)00033-X.

[4] Eisbruch A, Kim HM, Terrell JE, Marsh LH, Dawson LA, Ship JA. Xerostomia and its predictors following parotid-sparing irradiation of head-and-neck cancer. Int J Radiat Oncol Biol Phys 2001;50:695–704. https://doi.org/10.1016/S0360-3016(01)01512-7.

[5] Cheng SCH, Wu VWC, Kwong DLW, Ying M. Assessment of post-radiotherapy salivary glands. Br J Radiol 2011;84:393–402. https://doi.org/10.1259/bjr/66754762.

[6] Meirovitz A, Murdoch-Kinch CA, Schipper M, Pan C, Eisbruch A. Grading xerostomia by physicians or by patients after intensity-modulated radiotherapy of head-and-neck cancer. Int J Radiat Oncol Biol Phys 2006;66:445–53. https://doi.org/10.1016/j.ijrobp.2006.05.002.

[7] Wilkie JR, Mierzwa ML, Yao J, Eisbruch A, Feng M, Weyburne G, et al. Big data analysis of associations between patient reported outcomes, observer reported toxicities, and overall quality of life in head and neck cancer patients treated with radiation therapy. Radiother Oncol 2019;137:167–74. https://doi.org/10.1016/j.radonc.2019.04.030.

[8] Deasy JO, Moiseenko V, Marks L, Chao KSC, Nam J, Eisbruch A. Radiotherapy dose-volume effects on salivary gland function. Int J Radiat Oncol Biol Phys 2010;76:S58–63. https://doi.org/10.1016/j.ijrobp.2009.06.090.

[9] Murdoch-Kinch CA, Kim HM, Vineberg KA, Ship JA, Eisbruch A. Dose-effect relationships for the submandibular salivary glands and implications for their sparing by intensity modulated radiotherapy. Int J Radiat Oncol Biol Phys 2008;72:373–82. https://doi.org/10.1016/j.ijrobp.2007.12.033.

[10] Klein Nulent TJW, Valstar MH, de Keizer B, Willems SM, Smit LA, Al-Mamgani A, et al. Physiologic distribution of PSMA-ligand in salivary glands and seromucous glands of the head and neck on PET/CT. Oral Surg, Oral Med, Oral Pathol Oral Radiol 2018;125:478–86. https://doi.org/10.1016/j.oooo.2018.01.011.

[11] Valstar MH, Owers EC, Al-Mamgani A, Smeele LE, van de Kamer JB, Sonke JJ, et al. Prostate-specific membrane antigen positron emission tomography/computed tomography as a potential tool to assess and guide salivary gland irradiation. Phys Imaging Radiat Oncol 2019;9:65–8. https://doi.org/10.1016/j.phro.2019.02.004.

[12] Beetz I, Burlage FR, Bijl HP, Hoegen-Chouvalova O, Christianen MEMC, Vissink A, et al. The groningen radiotherapy-induced xerostomia questionnaire: development and validation of a new questionnaire. Radiother Oncol 2010;97:127–31. https://doi.org/10.1016/j.radonc.2010.05.004.

[13] Mencarelli A, Van Kranen SR, Hamming-Vrieze O, Van Beek S, Nico Rasch CR, Van Herk M, et al. Deformable image registration for adaptive radiation therapy of head and neck cancer: accuracy and precision in the presence of tumor changes. Int J Radiat Oncol Biol Phys 2014;90:680–7. https://doi.org/10.1016/j.ijrobp.2014.06.045.

[14] R Core Team / R Foundation for Statistical Computing. R: A Language and Environment for Statistical Computing 2021.

[15] Bates D, Mächler M, Bolker BM, Walker SC. Fitting linear mixed-effects models using lme4. J Stat Softw 2015:67. https://doi.org/10.18637/jss.v067.i01.
[16] Wickham H. ggplot2: Elegant Graphics for Data Analysis. New York: Springer-Verlag; 2016.
[17] Long JA. interactions: Comprehensive, User-Friendly Toolkit for Probing Interactions 2019.
[18] Xu R. Measuring explained variation in linear mixed effects models. Stat Med 2003;22:3527–41. https://doi.org/10.1002/sim.1572.
[19] Buus S, Grau C, Munk OL, Rodell A, Jensen K, Mouridsen K, et al. Individual radiation response of parotid glands investigated by dynamic 11C-methionine PET. Radiother Oncol 2006;78:262–9. https://doi.org/10.1016/j.radonc.2006.02.013.
[20] Roach MC, Turkington TG, Higgins KA, Hawk TC, Hoang JK, Brizel DM. FDG-PET assessment of the effect of head and neck radiotherapy on parotid gland glucose metabolism. Int J Radiat Oncol Biol Phys 2012;82:321–6. https://doi.org/10.1016/j.ijrobp.2010.08.055.
[21] Cannon B, Schwartz DL, Dong L. Metabolic imaging biomarkers of postradiotherapy xerostomia. Int J Radiat Oncol Biol Phys 2012;83:1609–16. https://doi.org/10.1016/j.ijrobp.2011.10.074.
[22] van Dijk LV, Noordzij W, Brouwer CL, Boellaard R, Burgerhof JGM, Langendijk JA, et al. 18F-FDG PET image biomarkers improve prediction of late radiation-induced xerostomia. Radiother Oncol 2018;126:89–95. https://doi.org/10.1016/j.radonc.2017.08.024.
[23] Wilkie JR, Mierzwa ML, Casper KA, Mayo CS, Schipper MJ, Eisbruch A, et al. Predicting late radiation-induced xerostomia with parotid gland PET biomarkers and dose metrics. Radiother Oncol 2020;148:30–7. https://doi.org/10.1016/j.radonc.2020.03.037.
[24] Elhalawani H, Cardenas CE, Volpe S, Barua S, Stieb S, Rock CB, et al. 18FDG positron emission tomography mining for metabolic imaging biomarkers of radiation-induced xerostomia in patients with oropharyngeal cancer. Clin Transl Radiat Oncol 2021;29:93–101. https://doi.org/10.1016/j.ctro.2021.05.011.
[25] Mouminah A, Borja AJ, Hancin EC, Chang YC, Werner TJ, Swisher-McClure S, et al. 18F-FDG-PET/CT in radiation therapy-induced parotid gland inflammation. Eur J Hybrid Imaging 2020:4. https://doi.org/10.1186/s41824-020-00091-x.
[26] olde Heuvel J, de Wit-van der Veen BJ, Donswijk ML, Slump CH, Stokkel MPM. Day-to-day variability of [68Ga]Ga-PSMA-11 accumulation in primary prostate cancer: effects on tracer uptake and visual interpretation. EJNMMI Res 2020:10. https://doi.org/10.1186/s13550-020-00708-z.
[27] Vickers AJ. The use of percentage change from baseline as an outcome in a controlled trial is statistically inefficient: a simulation study. BMC Med Res Method 2001;1:1–4. https://doi.org/10.1186/1471-2288-1-6.
[28] Gupta T, Hotwani C, Kannan S, Master Z, Rangarajan V, Murthy V, et al. Prospective longitudinal assessment of parotid gland function using dynamic quantitative pertechnate scintigraphy and estimation of dose-response relationship of parotid-sparing radiotherapy in head-neck cancers. Radiat Oncol 2015;10:1–9. https://doi.org/10.1186/s13014-015-0371-2.
[29] Dijkema T, Raaijmakers CPJ, ten Haken RK, Roesink JM, Braam PM, Houweling AC, et al. Parotid gland function after radiotherapy: the combined Michigan and Utrecht experience. Int J Radiat Oncol Biol Phys 2010;78:449–53. https://doi.org/10.1016/j.ijrobp.2009.07.1708.
[30] Murthy V, Lewis S, Kannan S, Khadanga CR, Rangarajan V, Joshi K, et al. Submandibular function recovery after IMRT in head and neck cancer: a prospective dose modelling study. Radiother Oncol 2018;129:38–43. https://doi.org/10.1016/j.radonc.2018.02.021.
[31] Shinta FDAI, Dinar N, Susanto H, Agustina D. Unstimulated salivary flow rate corresponds with severity of xerostomia: evaluation using xerostomia questionnaire and groningen radiotherapy- induced xerostomia questionnaire. J Dent Indonesia 2014:21. https://doi.org/10.14693/jdi.v0i0.187.
[32] Steenbakkers RJHM, van Rijn-Dekker MI, Stokman MA, Kierkels RGJ, van der Schaaf A, van den Hoek JGM, et al. Parotid gland stem cell sparing radiation therapy for patients with head and neck cancer: a double-blinded randomized controlled trial. Int J Radiat Oncol Biol Phys 2022;112:306–16. https://doi.org/10.1016/j.ijrobp.2021.09.023.